



# A re-assessment of nickel-doping method in iron isotope analysis on rock samples using multi-collector inductively coupled plasma mass spectrometry

Hongmei Gong<sup>1,2</sup> · Pengyuan Guo<sup>1,2,5</sup> · Shuo Chen<sup>1,2</sup> · Meng Duan<sup>1,2</sup> · Pu Sun<sup>1,2</sup> · Xiaohong Wang<sup>1,2</sup> · Yaoling Niu<sup>1,2,3,4</sup>

Received: 31 May 2019/Revised: 18 October 2019/Accepted: 17 December 2019

© Science Press and Institute of Geochemistry, CAS and Springer-Verlag GmbH Germany, part of Springer Nature 2020

**Abstract** Element doping has been proved to be a useful method to correct for the mass bias fractionation when analyzing iron isotope compositions. We present a systematic re-assessment on how the doped nickel may affect the iron isotope analysis in this study by carrying out several experiments. We find three important factors that can affect the analytical results, including the Ni:Fe ratio in the analyte solutions, the match of the Ni:Fe ratio between the unknown sample and standard solutions, and the match of the Fe concentration between the sample and standard solutions. Thus, caution is required when adding Ni to the analyte Fe solutions before analysis. Using our method, the  $\delta^{56}\text{Fe}$  and  $\delta^{57}\text{Fe}$  values of the USGS standards W-2a, BHVO-2, BCR-2, AGV-2 and GSP-2 are consistent with the recommended literature values, and the long-term (one year) external reproducibility is better than 0.03 and 0.05‰ (2SD) for  $\delta^{56}\text{Fe}$  and  $\delta^{57}\text{Fe}$ , respectively. Therefore, the analytical method established in our laboratory is a method

of choice for high quantity Fe isotope data in geological materials.

**Keywords** Fe isotope · Ni-doping · Stable isotope · Precision and accuracy · Mass bias correction · Pseudo-high mass resolution

## 1 Introduction

With the development of the multi-collector inductively coupled plasma mass spectrometry (MC ICP-MS) and improved analytical procedures, Fe isotope data of high precision and accuracy on rock samples can be acquired (Dauphas et al. 2017). These data allow studying possible Fe isotopic fractionation during high-temperature geological processes on Earth and other planets (e.g., Williams and Bizimis 2014; Sossi et al. 2016), such as partial melting (e.g., Weyer et al. 2005; Weyer and Ionov 2007), mantle metasomatism (e.g., Zhao et al. 2010, 2012, 2015; Huang et al. 2011; Poitrasson et al. 2013) and magma evolution (e.g., Teng et al. 2008; Zambardi et al. 2014). However, available iron isotope data still cannot yet be used effectively to trace petrogenic processes until possible mechanisms of iron isotope fractionation are fully understood. The latter still requires more high-quality Fe isotope data on various Earth materials, especially on rocks and minerals of known origin, to discover systematics towards genuine understanding mechanisms of Fe isotope fractionation in geological processes.

Nevertheless, there are analytical challenges in obtaining high-quality Fe isotope data such as polyatomic ion interferences and instrumental mass bias. The polyatomic ion interferences can be overcome using the high mass resolution on Nu Plasma 1700 or pseudo-high mass

✉ Pengyuan Guo  
guopy@qdio.ac.cn

<sup>1</sup> Key Laboratory of Marine Geology and Environment, Institute of Oceanology, Chinese Academy of Sciences, Qingdao 266071, China

<sup>2</sup> Qingdao National Laboratory for Marine Science and Technology, Qingdao 266061, China

<sup>3</sup> Department of Earth Sciences, Durham University, Durham DH1 3LE, UK

<sup>4</sup> School of Earth Science and Resources, China University of Geosciences, Beijing 100083, China

<sup>5</sup> Present Address: Institute of Oceanology, Chinese Academy of Sciences, Nanhai Road 7, Qingdao 266071, Shandong, China

resolution on Nu Plasma II and Neptune Plus by effectively separating the interfering ions from Fe ions and measuring the left flat-top peak sections of Fe isotopes. This is because the Fe isotopes have a lower mass relative to the polyatomic interferences, so Fe isotopes enter the detector first in a scan and form the left plateau. The center plateau consists of polyatomic interferences and the Fe isotopes, while the right plateau reflects the polyatomic interferences only. The instrumental mass biases can be corrected by using one of the three common methods, i.e., standard-sample bracketing (SSB) (e.g., He et al. 2015; Liu et al. 2014; Weyer and Schwieters 2003), double spike (e.g., Finlayson et al. 2015; Millet et al. 2012), and element doping (e.g., Arnold et al. 2004; Chen et al. 2017a; Dauphas et al. 2009; Sossi et al. 2015). The SSB method, the most often used method, assumes that mass bias during sample measurements is the same as bracketing standard measurements. But this method requires a well-controlled laboratory environment (e.g., temperature, humidity, air exhausting rate), instrument stability as well as the highly matched matrix. The isotopic double spike method (e.g., Malinovsky et al. 2003; Millet et al. 2012) is not sensitive to laboratory conditions as is the SSB method because the double-spike method can readily correct for instrument mass fractionation. This method is also proved to be able to produce the most precise Fe isotopic data to date (2SD = 0.02 ‰;  $N = 51$ ; Millet et al. 2012). However, the iterative computation of this method is very complex. In this case, internal elemental doping is the method of choice, assuming that the isotopes of the doped element have similar mass fractionation behavior to isotopes of the element of interest.

For iron isotope analysis, copper or nickel is usually used as the internal standard element for mass bias correction. Because the mass dispersion on the instrument is insufficient to simultaneously collect masses  $^{54}\text{Fe}$  to  $^{65}\text{Cu}$ , when Cu is used as an internal standard, the Cu and Fe isotopes cannot be analyzed in one cycle (i.e., at one magnet scan). In this case, the dynamic mode of the two-sequence analysis must be used, which requires extended analysis time and has the potential problem of the magnet inability to achieve stable signals. Thus, nickel is considered as a more suitable internal standard element for mass bias correction for Fe isotope analysis.

In this paper, we present new experimental results on Ni-doping method of iron isotope analysis using pseudo-high mass resolution on Nu Plasma II MC ICP-MS with wet plasma condition. We analyze the effects of Ni/Fe ratio, the match of Ni:Fe ratio between the sample and standard solutions, and the match of Fe concentrations between the sample and standard solutions. These former two variables are crucial to the accuracy of the iron isotope analysis, while the latter one is somewhat not that harsh,

which is an obvious advantage compared with the SSB method. Therefore, caution is necessary when using the internal standard doping method. The analyzed Fe isotopic compositions of the USGS reference materials using this method are in good agreement with the recommended values within error. On the basis of repeated analysis over one year's period, the precision and reproducibility of an in-house standard Alfa Fe solution are  $\pm 0.03$  ‰ (2SD) and  $\pm 0.05$  ‰ (2SD) for  $\delta^{56}\text{Fe}$  and  $\delta^{57}\text{Fe}$ , respectively.

## 2 Analytical methods

### 2.1 Sample digestion

The sample digestion method used in this study is modified from Chen et al. (2017b). Briefly, sample powders (5–10 mg) are weighted in a 10 mL PFA Teflon vial with a successive addition of 1 mL of 3:1 acid mixture of concentrated  $\text{HNO}_3$  +  $\text{HCl}$  and 0.5 mL of concentrated HF. The Teflon vials are then sealed in a high-pressure bomb for 15 h at 190 °C. The sample solutions are then evaporated to incipient dryness at 100 °C, refluxed with 2 mL of concentrated  $\text{HNO}_3$  before being heated again to incipient dryness to remove all the residual HF. The samples are then re-dissolved in 3 N distilled  $\text{HNO}_3$  for 2 h till complete digestion/dissolution. Finally, the samples are dried again and dissolved in 1 mL of 9 N HCl on a hotplate.

### 2.2 Chromatography procedure

The method of elemental separation and purification follows Cheng et al. (2014) with modification. Polyethylene columns with a length of 4.0 cm and an internal column diameter of 0.8 cm are filled with 1.0 mL of Bio-Rad® AG-MP-1 M resin (200–400 mesh). The resin filled columns are pre-cleaned by eluting 5 mL of Milli-Q water (18.2 M $\Omega$ ), 5 mL of 1 N HCl and 5 mL of 9 N HCl through the columns, successively (Table 1), where the 9 N HCl both cleans and equilibrates the resin by converting it into a chloride form. The HCl used in the whole procedures is double purified using a Savillex DST-1000 sub-boiling distillation system. Sample solutions in 1 mL of 9 N HCl are loaded into the columns, followed by 5 mL of 9 N HCl and 5 mL of 6 N HCl to fully elute matrix elements (e.g., Na, Mg, Al, Ca, Ti, Cr, Ni, Mn, Co) (Fig. 1). 0.5 mL of 1 N HCl is then added into the columns, during which ferric chlorides in solutions are visible as a thin yellow ring on the resin migrating from the top to the middle of the columns. Iron fraction was then completely eluted by the following 1.5 mL of 1 N HCl and collected in Teflon beakers (Table 1 and Fig. 1). The yields

**Table 1** Column chromatography procedure for Fe purification

No.	Step	Solvent	Note
1	Cleaning	5 ml Milli-Q	
2	Cleaning	5 ml 1 N HCl	
3	Cleaning/conditioning	5 ml 9 N HCl	
4	Sample loading	1 ml 9 N HCl	Totally digested sample
5	Eluting matrix	5 ml 9 N HCl	
6	Eluting matrix	5 ml 6 N HCl	
7	Eluting matrix	0.5 ml 1 N HCl	Visibly, a yellow coloration on the resin migrated from the top to the middle of the column
8	Collecting Fe	1.5 ml 1 N HCl	The ferric in chloride form, with yellow coloration visibly on the resin, were eluted down and collected into beakers
9	Cleaning	5 ml 1 N HCl	
10	Cleaning	5 ml Milli-Q	

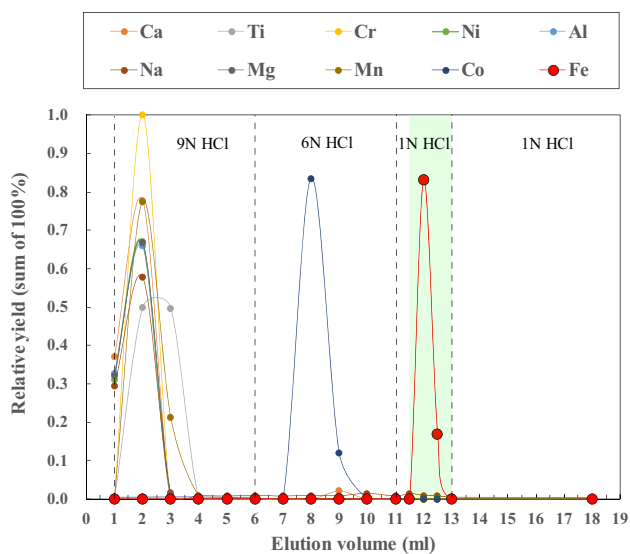


**Fig. 1** Elution curves for USGS rock standard BCR-2 on a 1 mL resin bed of AG-MP-1 M. The light green band stands for Fe collection

of Fe are always > 99.5 %. Total procedural blank for Fe were routinely measured and give a long-term average of 79 ng (N = 16), which is less than ~ 0.01 % of the processed samples and thus are considered negligible.

### 2.3 Mass spectrometry

Iron isotope analysis is done in the Laboratory of Ocean Lithosphere and Mantle Dynamics, Institute of Oceanology, Chinese Academy of Sciences, using a Nu Plasma II MC-ICP-MS equipped with 16 Faraday cups connected to an array of  $10^{11} \Omega$  resistor amplifiers in static mode. The introduction of Fe solution consists of a 100  $\mu\text{L}/\text{min}$  MicroMist nebulizer (Glass Expansion, Australia) connected to a Scott double-pass quartz cyclonic spray

chamber, and paired skimmer cone + sampling cone made from nickel. Such a setup of wet plasma facilitates greater stability than using desolvation nebulizer of dry plasma (Dauphas et al. 2009).

Iron isotopic ratios are measured in pseudo-high resolution mode using the 50  $\mu\text{m}$  width source slit and alpha slits in order to correct for beam aberrations. The instrumental parameters are fully tuned to ensure mass resolution better than 7500 for data acquisition. During the measurement,  $\text{Fe}^+$  peaks were resolved from interfering  $\text{ArO}^+$ ,  $\text{ArOH}^+$  and  $\text{ArN}^+$  isobars as flat-topped plateaus on the low mass shoulder of argide peaks (Weyer and Schwieters 2003).  $^{54}\text{Fe}$ ,  $^{56}\text{Fe}$ ,  $^{57}\text{Fe}$ ,  $^{58}(\text{Fe}, \text{Ni})$ ,  $^{60}\text{Ni}$  and  $^{61}\text{Ni}$  isotopes were simultaneously collected by Faraday cups at Low 6, Low 3, Central, High 3, High 8 and High 9 positions, respectively, on our Nu Plasma II instrument (see Table 2). Sample solutions were “spiked” with GSB Ni (an ultrapure single-elemental standard solution from the China Iron and Steel Research Institute, SN: 18040213) for mass fractionation correction. Before that, each sample solution is scanned using Inductively Coupled Plasma Optical Emission Spectrometer (ICP-OES) prior to Fe isotopes analysis to ensure no detectable Cr and Ni. This is because  $^{54}\text{Cr}$  would interfere  $^{54}\text{Fe}$  and Ni compositions of the doped GSB Ni solution would be somewhat changed if any matrix Cr and Ni remain in the purified solutions. In our experiment, the Fe concentration of analyte solution is usually  $\geq 12$  ppm, corresponding to a ~ 20 V total Fe signal, which is necessary to obtain high-precision iron isotopic results. Data acquisition was performed in one block of 30 measurements, and a total 570 s was required for one analysis. Considering the possible slightly magnet drift, peak centering (magnet centering at a given offset from the bottom of the peak) were carried out before each block. To obtain the high precision data, each sample was repeated at

**Table 2** Faraday cup configuration used for the iron isotope measurements by Nu Plasma II MC-ICP-MS

Nominal mass	54	56	57	58	60	61
Measured element	Fe (5.80 %)	Fe (91.72 %)	Fe (2.20 %)	Fe (0.28 %)		
Mass bias correcting element				Ni (68.08 %)	Ni (26.22 %)	Ni (1.14 %)
Faraday cup used	L6	L3	Central	H3	H8	H9

least four times after a standard analysis, and the reported isotopic compositions are the averages of repeated analyses. More details of the instrumental working parameters are listed in Table 3.

During the analysis process, the instrumental mass bias is corrected using simultaneously determined  $^{58}\text{Ni}$  and  $^{60}\text{Ni}$  in the sample solution doped with a GSB Ni solution, combined with an exponential law as below:

$$\left[\frac{^{56}\text{Fe}}{^{54}\text{Fe}}\right]_T = \left[\frac{^{56}\text{Fe}}{^{54}\text{Fe}}\right]_M \times \left[\frac{^{56}\text{Mass}(\text{Fe})}{^{54}\text{Mass}(\text{Fe})}\right]^{\beta_1} \quad (1)$$

$$\left[\frac{^{60}\text{Ni}}{^{58}\text{Ni}}\right]_T = \left[\frac{^{60}\text{Ni}}{^{58}\text{Ni}}\right]_M \times \left[\frac{^{60}\text{Mass}(\text{Ni})}{^{58}\text{Mass}(\text{Ni})}\right]^{\beta_2} \quad (2)$$

where  $\beta_1$ ,  $\beta_2$  represent the mass bias fractionation factors for Fe and Ni isotopes, and  $T$ ,  $M$  denote true and measured isotope ratios, respectively. In our correction, we use the natural Ni isotopic abundance ratios  $\left[\frac{^{60}\text{Mass}(\text{Ni})}{^{58}\text{Mass}(\text{Ni})}\right]_T = 0.385199$  (Gramlich et al. 1989) and assume  $\beta_1 = \beta_2$ . Note that the  $^{58}\text{Ni}$  here is  $^{58}\text{Fe}$  corrected, i.e.,

$$^{58}\text{Ni} = ^{58}\text{Total} - ^{58}\text{Fe} = ^{58}\text{Total} - ^{56}\text{Fe} \times 0.003074 \quad (3)$$

given  $^{58}\text{Fe}/^{56}\text{Fe} = 0.003074$  following Taylor et al. (1992). For comparison, we also conduct the mass bias fractionation correction using  $^{61}\text{Ni}$  and  $^{60}\text{Ni}$  (see below).

The Fe isotopic data are reported in standard  $\delta$  notation in per mil relative to the standard reference material (IRMM-014; Taylor et al. 1992):

$$\delta^{56}\text{Fe}_{\text{IRMM-014}} = \left[ \left( \frac{^{56}\text{Fe}/^{54}\text{Fe}}{^{56}\text{Fe}/^{54}\text{Fe}} \right)_{\text{sample}} / \left( \frac{^{56}\text{Fe}/^{54}\text{Fe}}{^{56}\text{Fe}/^{54}\text{Fe}} \right)_{\text{IRMM-014}} \right] \times 1000$$

$$\delta^{57}\text{Fe}_{\text{IRMM-014}} = \left[ \left( \frac{^{57}\text{Fe}/^{54}\text{Fe}}{^{57}\text{Fe}/^{54}\text{Fe}} \right)_{\text{sample}} / \left( \frac{^{57}\text{Fe}/^{54}\text{Fe}}{^{57}\text{Fe}/^{54}\text{Fe}} \right)_{\text{IRMM-014}} \right] \times 1000$$

Because of the lack of IRMM-014 in our laboratory, we used GSB Fe solution (from He et al. 2015) as the replacement in this study, with transformation of  $\delta^{56}\text{Fe}_{\text{GSB}} = \delta^{56}\text{Fe}_{\text{IRMM-014}} - 0.729$  and  $\delta^{57}\text{Fe}_{\text{GSB}} = \delta^{57}\text{Fe}_{\text{IRMM-014}} - 1.073$  within error of 0.03‰ (2SD).

## 3 Results and Discussion

### 3.1 The feasibility of Ni-doping method for mass bias corrections

Before we evaluate the feasibility of Ni-doping method to correct the instrument mass bias fractionation, we need to choose which two of the Ni isotopes' ratio is more reliable to calculate the fractionation factor. As reported previously, both  $^{60}\text{Ni}/^{58}\text{Ni}$  (Chen et al. 2017a) and  $^{61}\text{Ni}/^{60}\text{Ni}$  (Poitrasson & Freydier 2005) have been adopted and both methods can produce data with good precision and accuracy. In our case, we prefer  $^{60}\text{Ni}/^{58}\text{Ni}$  than  $^{61}\text{Ni}/^{60}\text{Ni}$ . Figure 2 compares the long-term (Jan. to Apr. 2019) measured mass bias fractionation factors for Fe and Ni isotopic ratios obtained through the analyses of the Alfa Fe solution and the GSB Fe standard solution (He et al. 2015). Obviously, the correlation coefficients between  $\beta_{\text{Fe}56-54}$  and  $\beta_{\text{Ni}60-58}$  are much better than that of the  $\beta_{\text{Fe}56-54}$  and  $\beta_{\text{Fe}61-60}$  in both Alfa Fe and GSB Fe solutions, which implies using  $\beta_{\text{Ni}60-58}$  is more reliable to correct the Fe isotopes' mass bias fractionation. In Fig. 2, the Alfa Fe data define a linear trend with a slope of  $1.0126 \pm 0.0887$

**Table 3** Detailed information of the instrumental working parameters

Coolant gas	13.0 L/min
Auxiliary gas	0.9 L/min
Ar Nebulizer gas	35–36 psi
RF power	1300 W
Amplifier	$10^{11} \Omega$
Spray chamber	Scott double-pass quartz cyclonical
Sampling cone	Ni orifice, 325–294
Skimmer cone	Ni orifice, 319–497
Solution uptake	100 uL/min
Washing time	240 s
Transfer time	60 s
Integration time	240 s ( $30 \times 8$ s)
Background analysis	ESA deflection 30 s
Sensitivity	$\sim 1.7$ V/ppm (total Fe)

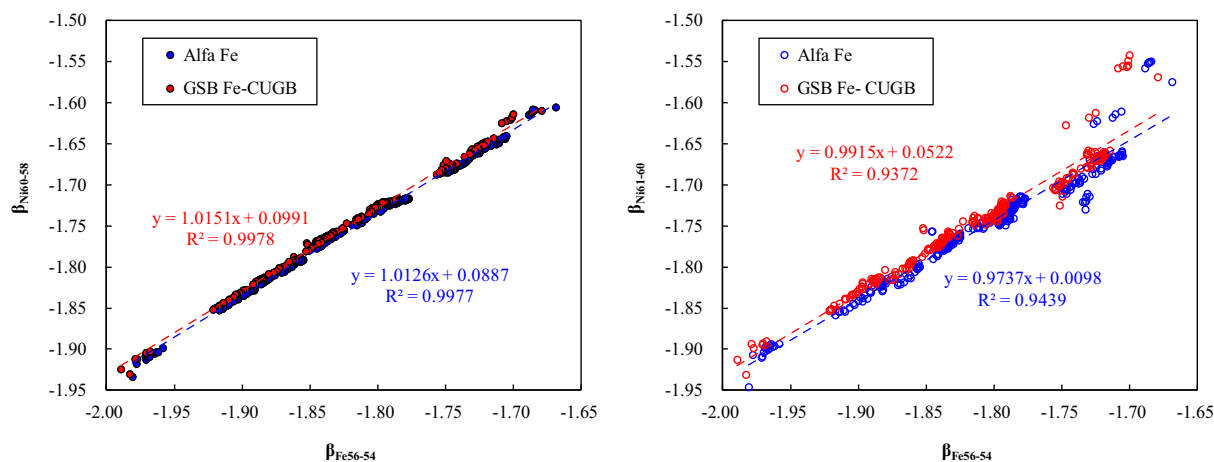


**Fig. 2** Plot of measured mass fractionation factors for Fe and Ni isotopic ratios obtained through analyses of the GSB Fe-CUGB and the Alfa Fe over the period of four months. Theoretical slope (TS) =  $\ln(\text{Mass}^{56}\text{Fe}/\text{Mass}^{54}\text{Fe})/\ln(\text{Mass}^{60}\text{Ni}/\text{Mass}^{58}\text{Ni}) = 1.073$

( $R^2 = 0.9977$ ,  $n = 281$ ), and the data by GSB Fe-CUGB defines a linear trend with a slope of  $1.0151 \pm 0.0991$  ( $R^2 = 0.9978$ ,  $n = 231$ ). This suggests that the mass bias fractionation factors are slightly different for iron and nickel in our instrument. However, both the above fractionation factors are identical to the theoretical slope within error (TS = 1.073, calculated assuming a natural mass weight of Fe and Ni). Furthermore, such a difference in mass bias factors would result in a maximum  $\sim 0.03\%$  inaccuracy for  $\delta^{56}\text{Fe}$  as discussed in Poitrasson and Freyrier (2005), which is comparable to our long-term precision ( $\pm 0.03\%$ , see below). Therefore, we assume that Ni and Fe have the same fractionation factor during the Fe isotope analysis in our case. In general, the experiment above justifies that the Ni-doping method is effective to correct for instrumental mass fractionation during the Fe isotope analysis.

### 3.2 The Ni:Fe ratio effect

In order to evaluate the effect of the Ni:Fe ratio in the sample solution on the Fe isotope analysis result, 14 ppm Alfa Fe solution was mixed with GSB Ni with Ni:Fe ratios ranging from  $\sim 0.1$  to  $\sim 3.0$ . In the experiment, the Ni:Fe ratios in the Alfa Fe solution and in the standard GSB Fe-CUGB were highly matched. The experimental results show that the  $\delta^{56}\text{Fe}$  values of the Alfa Fe solution increase with decreasing Ni:Fe ratios (Fig. 3), being consistent with the results in Chen et al. (2017a). According to our experimental results, the Alfa Fe solutions with Ni:Fe ratios ranging from 0.8 to 2.1 can yield accurate  $\delta^{56}\text{Fe}$  values. The Alfa Fe solutions with Ni:Fe ratio  $< 0.5$  yield  $\delta^{56}\text{Fe}$  values abnormally higher than reference values

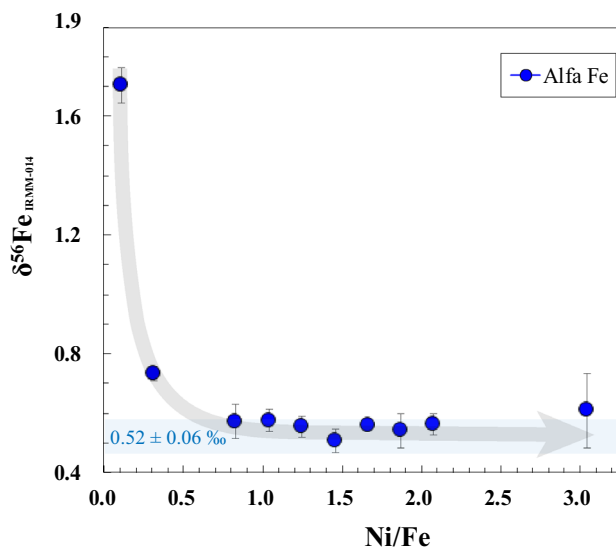


**Fig. 3** Effect of varying Fe/Ni ratio on Fe isotopic analyses. Error bars represent  $2\sigma$  uncertainties, and the light blue band denotes the recommended Fe isotopic values within  $2\sigma$  uncertainties, i.e.,  $0.52 \pm 0.06\%$

( $0.52 \pm 0.03\%$ ). The possible reason might be that low Ni intensity would increase the effect of  $^{58}\text{Fe}$  on  $^{58}\text{Ni}$ , which affect the mass bias fractionation factor in return and result in abnormally high  $\delta^{56}\text{Fe}$  as well. On the other hand, the data show that both the accuracy and precision when Ni:Fe  $> 3.0$  are not as good as that when Ni:Fe = 1.0–2.0, an explanation is that the high concentration of the Ni would suppress the Fe ionization at the touch position. In our laboratory, to achieve the best results, the Ni:Fe ratio in solutions is usually fixed at  $\sim 1.4$ – $1.5$ .

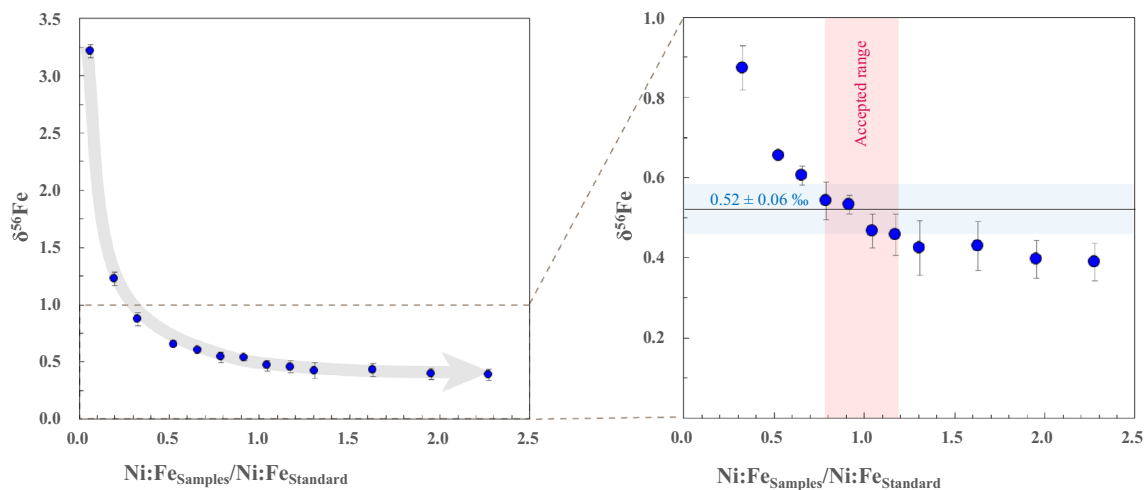


**Fig. 4** Effect of varying Fe/Ni ratio between sample and standard. Error bars represent  $2\sigma$  uncertainties. The light blue band denotes the recommended Fe isotopic values within  $2\sigma$  uncertainties, i.e.,  $0.52 \pm 0.06 \text{ ‰}$ , and the light red area denotes the accepted relative difference in Ni:Fe ratios between samples and standard in our lab

### 3.3 The match of Ni:Fe ratios between samples and standard solutions

The match of Ni:Fe ratios between samples and standards is also an important variable that affects the data. This is because the mismatch of the Ni:Fe ratio between samples and standards solutions would result in different mass bias in the instrument. To explore the effect of the Ni:Fe ratio match between samples and standard, we fixed the Ni:Fe ratio in the standard (GSB Fe-CUGB) at 1.58 with 12 ppm Fe concentration. At a given Fe concentration of 12 ppm in Alfa Fe solutions, the Ni:Fe ratios vary from 0.1 to 3.5. The data show that the  $\delta^{56}\text{Fe}$  values of the Alfa Fe solution increase with the  $\text{Ni:Fe}_{\text{standard}}/\text{Ni:Fe}_{\text{samples}}$  increasing (Fig. 4). That is, the mismatch of the Ni:Fe ratios between

the samples and the standard would greatly affect the analyzed results. For the purpose of accuracy in our laboratory, the recommended difference of Ni:Fe ratios between samples and standards (e.g.,  $\text{Ni:Fe}_{\text{standard}} - \text{Ni:Fe}_{\text{samples}}$ ) is less than 20 % in percentage.

### 3.4 The match of Fe concentration between samples and standards solutions

As we have demonstrated above, both the Ni:Fe ratio in analyte solutions and match of Ni:Fe ratio between samples and standards solutions are important to ensure good results. However, concentration effects, which refer to the changes in the instrumental mass bias (fractionation factor) with the concentrations of elements in the samples or

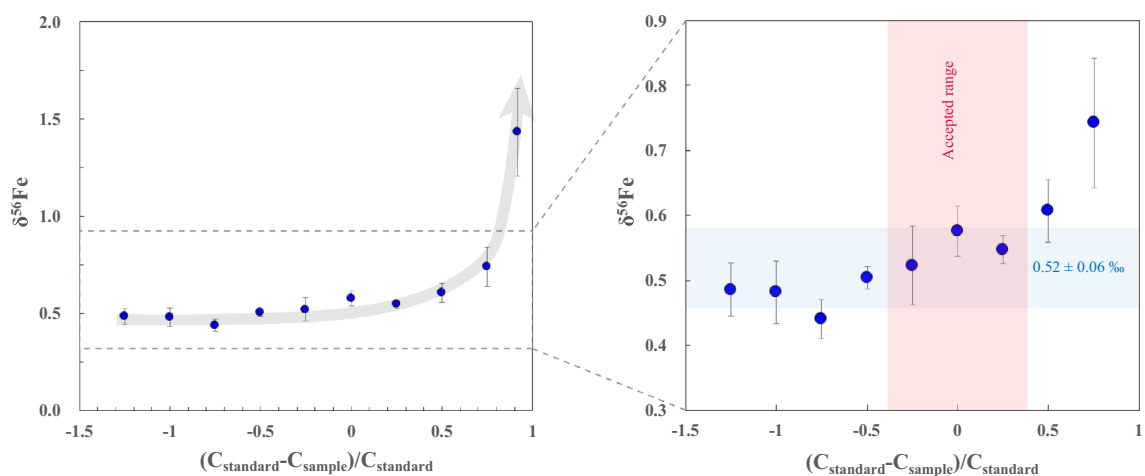


**Fig. 5** Effect of varying Fe concentration between sample and standard. Error bars represent  $2\sigma$  uncertainties. The light blue band denotes the recommended Fe isotopic values within  $2\sigma$  uncertainties, i.e.,  $0.52 \pm 0.06 \text{ ‰}$ , and the light red band denotes the accepted Fe concentration between samples and standard in our lab

**Fig. 6** Long-term stability of Fe isotopic compositions of the Alfa Fe. Bars represent 2SD

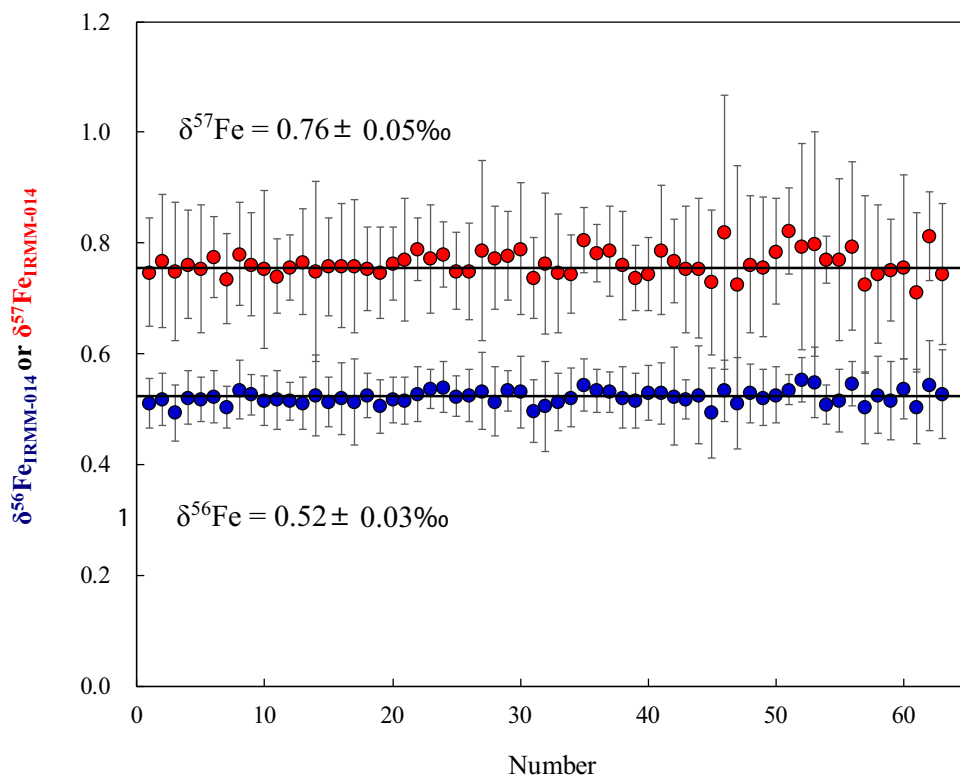
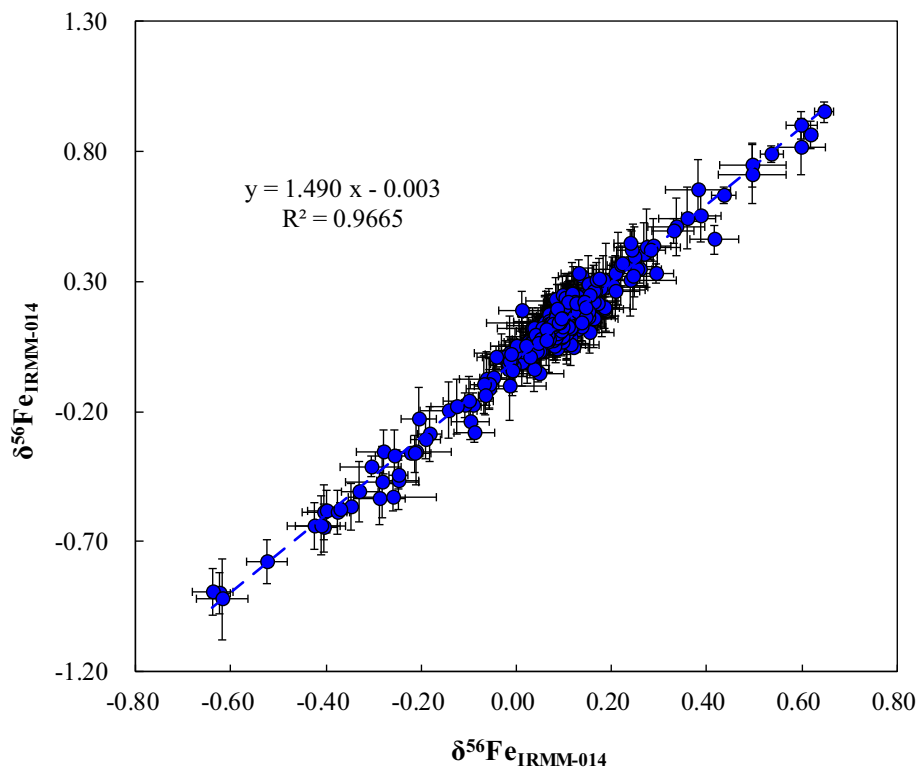


**Fig. 7** Iron isotope compositions of various geological samples relative to IRMM-014 analyzed over the period of three months. The gray line represents a linear regression of  $\delta^{56}\text{Fe}$  vs.  $\delta^{57}\text{Fe}$  with a slope of  $1.490 \pm 0.015$  (SE) ( $R^2 = 0.9665$ ,  $N = 332$ ). This relationship is statistically consistent with both theoretical predictions of mass-dependent isotope fractionation (slope of 1.475; Young et al. 2002) and with previously measured isotopic mass-dependent fractionation trends using Nu Plasma (slope of 1.482; Chen et al. 2017a)



standard during analysis, is also a key to obtain high-quality data (Zhu et al. 2002; Chen et al. 2017a). For the SSB method, the concentration match between samples and

standards is extremely important (Zhu et al. 2002). A previous study shows that the concentrations of the samples and the standards differ by more than 15 % would result in

**Table 4** Fe isotopic composition of USGS rock materials and geostandards reported in this study

Sample	Session	$\delta^{56}\text{Fe}$	2SD	$\delta^{57}\text{Fe}$	2SD	N
BHVO-2	1	0.11	0.03	0.16	0.07	4
	2	0.14	0.04	0.23	0.04	5
	3	0.14	0.06	0.22	0.11	5
	4	0.13	0.07	0.21	0.10	12
	5	0.11	0.02	0.16	0.04	8
	6	0.08	0.05	0.12	0.11	17
	7	0.11	0.03	0.13	0.14	6
	8	0.11	0.02	0.17	0.06	5
	9	0.08	0.01	0.12	0.03	5
	10	0.11	0.04	0.17	0.07	10
	11	0.09	0.04	0.15	0.09	4
	Averaged value	0.11	0.04	0.17	0.08	
	Craddock and Dauphas (2010)	0.11	0.01	0.17	0.02	
	He et al. (2015)	0.11	0.03	0.16	0.06	
Chen et al. (2017a)	0.10	0.03	0.15	0.06		
BCR-2	1	0.09	0.03	0.19	0.05	15
	2	0.08	0.04	0.15	0.04	5
	3	0.12	0.05	0.18	0.14	19
	4	0.06	0.03	0.09	0.02	4
	5	0.13	0.02	0.18	0.05	5
	6	0.06	0.04	0.07	0.09	5
	7	0.07	0.04	0.09	0.07	21
	8	0.08	0.02	0.12	0.04	12
	9	0.07	0.04	0.12	0.04	9
	10	0.07	0.04	0.09	0.07	5
	11	0.07	0.04	0.11	0.04	5
	12	0.10	0.03	0.10	0.11	5
	13	0.08	0.03	0.10	0.11	4
	Averaged value	0.08	0.04	0.12	0.08	
Craddock and Dauphas (2010)	0.09	0.01	0.13	0.02		
He et al. (2015)	0.08	0.03	0.13	0.05		
Chen et al. (2017a)	0.09	0.02	0.13	0.04		
AGV-2	1	0.08	0.02	0.09	0.03	5
	2	0.09	0.06	0.15	0.04	5
	3	0.09	0.05	0.14	0.09	15
	4	0.10	0.02	0.15	0.04	4
	5	0.09	0.06	0.14	0.09	10
	6	0.08	0.05	0.11	0.08	6
	7	0.09	0.04	0.19	0.05	5
	8	0.08	0.05	0.13	0.10	5
	9	0.09	0.05	0.11	0.08	5
	Averaged value	0.09	0.01	0.14	0.06	
Craddock and Dauphas (2010)	0.11	0.08	0.17	0.03		
He et al. (2015)	0.10	0.01	0.15	0.02		



**Table 4** continued

Sample	Session	$\delta^{56}\text{Fe}$	2SD	$\delta^{57}\text{Fe}$	2SD	N
GSP-2	1	0.13	0.05	0.19	0.10	14
	2	0.18	0.03	0.29	0.03	5
	3	0.14	0.03	0.20	0.08	5
	4	0.16	0.04	0.26	0.09	6
	5	0.13	0.04	0.24	0.08	5
	6	0.14	0.03	0.19	0.04	5
	Averaged value	0.15	0.04	0.23	0.08	
	Craddock and Dauphas (2010)	0.16	0.01	0.23	0.02	
Chen et al. 2017a	0.16	0.03	0.25	0.04		
W-2a	1	0.08	0.03	0.10	0.02	5
	2	0.05	0.04	0.06	0.06	5
	3	0.04	0.03	0.06	0.10	12
	4	0.05	0.03	0.07	0.05	8
	5	0.04	0.06	0.07	0.09	11
	6	0.04	0.06	0.09	0.08	14
	7	0.02	0.06	0.03	0.07	5
	Averaged value	0.05	0.03	0.07	0.04	
He et al. (2015)	0.05	0.03	0.05	0.08		
Alfa Fe	Long-term precision in our lab	0.52	0.03	0.76	0.05	63

Note: All the above analyte were digested and purified using the same procedure in our laboratory

a significant deviation between the measured and true values (Chen et al. 2017a). In our experiment, the Ni:Fe ratios in both samples and standard were fixed at 1.5. Given that the Fe concentration of the standard (GSB Fe) fixed at 12 ppm, we change the Fe concentration of Alfa Fe from 1 ppm to 27 ppm. The result shows that the  $\delta^{56}\text{Fe}$  values of Alfa Fe solution increase with  $(C_{\text{standard}} - C_{\text{sample}})/C_{\text{sample}}$  (Fig. 5), where  $C_{\text{standard}}$  stands for the concentration of the standard GSB Fe and  $C_{\text{sample}}$  stands for the concentration of the sample (Alfa Fe in our experiment). This suggests that the mismatch of Fe concentrations between samples and standards can also result in the measurement inaccuracy. In this case, we recommend that the Fe concentration difference by 40% between samples and standard is acceptable in our lab.

#### 4 Geological standards accuracy and precision check

To evaluate the accuracy and precision of Ni-doping method established in our laboratory, the Fe isotope composition of various samples have been measured and delta values were calculated relative to IRMM-014. One year analysis of an in-house standard Alfa Fe solution gives a long-term 2SD = 0.03 ‰ for  $\delta^{56}\text{Fe}$ , and 2SD = 0.05 ‰ for  $\delta^{57}\text{Fe}$  (Fig. 6). Figure 7 shows that the data form a linear trend between  $\delta^{56}\text{Fe}$  and  $\delta^{57}\text{Fe}$  with a slope of

$1.490 \pm 0.015$  (SE) ( $R^2 = 0.9665$ ,  $N = 332$ ), which is indistinguishable from theoretical predictions of mass-dependent isotope fractionation.

We analyzed USGS geological reference materials, including diabase (W-2a), basalt (BCR-2, BHVO-2), andesite (AGV-2) and granodiorite (GSP-2), during which the Fe concentration of these geological reference materials and standard (GSB Fe) solutions are  $\sim 12$ – $14$  ppm, with the Ni:Fe ratios well matched (i.e., Ni:Fe =  $\sim 1.4$ – $1.6$  in all analyte solutions). The results are reported in Table 4. The iron isotopic data obtained in this study are well consistent with the literature values within error (Craddock and Dauphas 2010 and references therein; Liu et al. 2014; He et al. 2015; Chen et al. 2017a; Li et al. 2019).

#### 5 Conclusion

To obtain high-quality Fe isotope data in laboratories, Ni-doping is the method of choice to effectively correct for the instrumental mass fractionation. However, caution is necessary when using this method. The Ni:Fe ratio should match well between samples and standards, while the Fe concentration match between samples and standards is not that rigorous. The Fe isotopic compositions of USGS rock materials determined using above Ni doping method are in good agreement with the literature data within 2SD uncertainties, and the precision and reproducibility of this

method are better than  $\pm 0.03$  ‰ (2SD, N = 63) for  $\delta^{56}\text{Fe}$  and better than  $\pm 0.05$  ‰ (2SD, N = 63) for  $\delta^{57}\text{Fe}$ , respectively.

**Acknowledgements** Yongsheng He kindly provided the GSB Fe standard solution. We thank Yue-xing Feng, Kaiyun Chen, Ming Li, Liang Li, Yajun An, Jin Li, Jianfeng Gao and Weiqiang Li for their help during our Fe analysis method establishing process. We acknowledge helpful reviews by the three anonymous reviewers. This work was supported by National Nature Science Foundation of China (Grant Numbers 41776067 and 41630968).

#### Compliance with ethical standards

**Conflict of interest** On behalf of all authors, the corresponding author states that there is no conflict of interest.

## References

- Arnold GL, Weyer S, Anbar AD (2004) Fe isotope variations in natural materials measured using high mass resolution multiple collector ICPMS. *Anal Chem* 76:322–327
- Chen KY, Yuan HL, Liang P, Bao ZA, Chen L (2017a) Improved nickel-corrected isotopic analysis of iron using high-resolution multi-collector inductively coupled plasma mass spectrometry. *Int J Mass Spectrom* 421:196–203
- Chen S, Wang X, Niu Y, Sun P, Duan M, Xiao Y, Xue Q (2017b) Simple and cost-effective methods for precise analysis of trace element abundances in geological materials with ICP-MS. *Sci Bull* 62(4):277–289
- Cheng T, Nebel O, Sossi PA, Chen F (2014) Refined separation of combined Fe–Hf from rock matrices for isotope analyses using AG-MP-1 M and Ln-Spec chromatographic extraction resins. *MethodsX* 1:144–150
- Craddock PR, Dauphas N (2010) Iron isotopic compositions of reference materials, geostandards and chondrites. *Geostand Geoanal Res* 35:101–123
- Dauphas N, Pourmand A, Teng F-Z (2009) Routine isotopic analysis of iron by HR-MC-ICPMS: How precise and how accurate? *Chem Geol* 267:175–184
- Dauphas N, John SG, Rouxel O (2017) Iron isotope systematics. *Rev Mineral Geochem* 82(1):415–510
- Finlayson VA, Konter JG, Ma L (2015) The importance of a Ni correction with ion counter in the double spike analysis of Fe isotope compositions using a  $^{57}\text{Fe}/^{58}\text{Fe}$  double spike. *Geochem Geophys Geosyst* 16:4209–4222
- Gramlich JW, Machlan LA, Barnes IL, Paulsen PJ (1989) Absolute isotopic abundance ratios and atomic weight of a reference sample of nickel. *J Res Nat Inst Stand Technol* 94:347–356
- He Y, Ke S, Teng F-Z, Wang T, Wu H, Lu Y, Li S (2015) High-precision iron isotope analysis of geological reference materials by high-resolution mc-icp-ms. *Geostand Geoanal Res* 39:341–356
- Huang F, Zhang Z, Lundstrom CC, Zhi X (2011) Iron and magnesium isotopic compositions of peridotite xenoliths from Eastern China. *Geochim Cosmochim Acta* 75:3318–3334
- Li J, Tang SH, Zhu XK, Li ZH, Li SZ, Yan B, Belshaw NS (2019) Basaltic and solution reference materials for iron, copper and zinc isotope measurements. *Geostand Geoanal Res* 43(00):163–175
- Liu S-A, Li D, Li S, Teng F-Z, Ke S, He Y, Lu Y (2014) High-precision copper and iron isotope analysis of igneous rock standards by MC-ICP-MS. *J Anal At Spectrom* 29:122–133
- Malinovsky D, Stenberg A, Rodushkin I, Andren H, Ingri J, Ohlander B, Baxter DC (2003) Performance of high resolution MC-ICP-MS for Fe isotope ratio measurements in sedimentary geological materials. *J Anal At Spectrom* 18:687–695
- Millet M-A, Baker JA, Payne CE (2012) Ultra-precise stable Fe isotope measurements by high resolution multiple-collector inductively coupled plasma mass spectrometry with a  $^{57}\text{Fe}$ – $^{58}\text{Fe}$  double spike. *Chem Geol* 304–305:18–25
- Poitrasson F, Freydier R (2005) Comment on “Heavy iron isotope composition of granites determined by high resolution MC-ICP-MS”, by F. Poitrasson and R. Freydier. *Chem Geol* 222(1–2):132–147
- Poitrasson F, Delpéch G, Grégoire M (2013) On the iron isotope heterogeneity of lithospheric mantle xenoliths: implications for mantle metasomatism, the origin of basalts and the iron isotope composition of the Earth. *Contrib Mineral Petrol* 165:1243–1258
- Sossi PA, Halverson GP, Nebel O, Eggins SM (2015) Combined separation of Cu, Fe and Zn from rock matrices and improved analytical protocols for stable isotope determination. *Geostand Geoanal Res* 39:129–149
- Sossi PA, Nebel O, Foden J (2016) Iron isotope systematics in planetary reservoirs. *Earth Planet Sci Lett* 452:295–308
- Taylor PDP, Maeck R, De Bièvre P (1992) Determination of the absolute isotopic composition and atomic weight of a reference sample of natural iron. *Int J Mass Spectrom Ion Processes* 121:111–125
- Teng FZ, Dauphas N, Helz RT (2008) Iron isotope fractionation during magmatic differentiation in Kilauea Iki lava lake. *Science* 320:1620–1622
- Weyer S, Ionov DA (2007) Partial melting and melt percolation in the mantle: the message from Fe isotopes. *Earth Planet Sci Lett* 259:119–133
- Weyer S, Schwieters J (2003) High precision Fe isotope measurements with high mass resolution MC-ICPMS. *Inter J Mass Spectrom* 226:355–368
- Weyer S, Anbar AD, Brey GP, Münker C, Mezger K, Woodland AB (2005) Iron isotope fractionation during planetary differentiation. *Earth Planet Sci Lett* 240:251–264
- Williams HM, Bizimis M (2014) Iron isotope tracing of mantle heterogeneity within the source regions of oceanic basalts. *Earth Planet Sci Lett* 404:396–407
- Young ED, Galy A, Nagahara H (2002) Kinetic and equilibrium mass-dependent isotope fractionation laws in nature and their geochemical and cosmochemical significance. *Geochim Cosmochim Acta* 66:1095–1104
- Zambardi T, Lundstrom CC, Li X, McCurry M (2014) Fe and Si isotope variations at Cedar Butte volcano; insight into magmatic differentiation. *Earth Planet Sci Lett* 405:169–179
- Zhao X, Zhang H, Zhu X, Tang S, Tang Y (2010) Iron isotope variations in spinel peridotite xenoliths from North China Craton: implications for mantle metasomatism. *Contrib Mineral Petrol* 160:1–14
- Zhao X, Zhang H, Zhu X, Tang S, Yan B (2012) Iron isotope evidence for multistage melt–peridotite interactions in the lithospheric mantle of eastern China. *Chem Geol* 292:127–139
- Zhao X, Zhang H, Zhu X, Zhu B, Cao H (2015) Effects of melt percolation on iron isotopic variation in peridotites from Yangyuan, North China Craton. *Chem Geol* 401:96–110
- Zhu X, Guo Y, Salvato B (2002) Mass fractionation processes of transition metal isotopes. *Earth Planet Sci. Lett.* 200:47–62